

See discussions, stats, and author profiles for this publication at: <https://www.researchgate.net/publication/6723775>

# Improving the Performance of a Quadrupole Time-of-Flight Instrument for Macromolecular Mass Spectrometry

ARTICLE *in* ANALYTICAL CHEMISTRY · DECEMBER 2006

Impact Factor: 5.64 · DOI: 10.1021/ac061039a · Source: PubMed

CITATIONS

129

READS

84

11 AUTHORS, INCLUDING:



**Esther van Duijn**

Utrecht University

30 PUBLICATIONS 1,500 CITATIONS

SEE PROFILE



**Kristina Lorenzen**

European XFEL

14 PUBLICATIONS 623 CITATIONS

SEE PROFILE



**John van der Oost**

Wageningen University

368 PUBLICATIONS 12,814 CITATIONS

SEE PROFILE



**Albert J R Heck**

Utrecht University

674 PUBLICATIONS 21,792 CITATIONS

SEE PROFILE

# Improving the Performance of a Quadrupole Time-of-Flight Instrument for Macromolecular Mass Spectrometry

Robert H. H. van den Heuvel,<sup>†</sup> Esther van Duijn,<sup>†</sup> Hortense Mazon,<sup>†</sup> Silvia A. Synowsky,<sup>†</sup> Kristina Lorenzen,<sup>†</sup> Cees Versluis,<sup>†</sup> Stan J. J. Brouns,<sup>‡</sup> Dave Langridge,<sup>§</sup> John van der Oost,<sup>‡</sup> John Hoyes,<sup>§</sup> and Albert J. R. Heck<sup>\*,†</sup>

Department of Biomolecular Mass Spectrometry, Bijvoet Center for Biomolecular Research and Utrecht Institute for Pharmaceutical Sciences, Utrecht University, Sorbonnelaan 16, 3584 CA Utrecht, The Netherlands, Laboratory of Microbiology, Wageningen University, Hesselink van Suchtelenweg 4, 6703 CT Wageningen, The Netherlands and MS Horizons, 34 Lea Road, Heaton Moor, Stockport, SK4 4JU, United Kingdom

We modified and optimized a first generation quadrupole time-of-flight (Q-TOF) 1 to perform tandem mass spectrometry on macromolecular protein complexes. The modified instrument allows isolation and subsequent dissociation of high-mass protein complexes through collisions with argon molecules. The modifications of the Q-TOF 1 include the introduction of (1) a flow-restricting sleeve around the first hexapole ion bridge, (2) a low-frequency ion-selecting quadrupole, (3) a high-pressure hexapole collision cell, (4) high-transmission grids in the multicomponent ion lenses, and (5) a low repetition rate pusher. Using these modifications, we demonstrate the experimental isolation of ions up to 12 800 mass-to-charge units and detection of product ions up to 38 150 Da, enabling the investigation of the gas-phase stability, protein complex topology, and quaternary structure of protein complexes. Some of the data reveal a so-far unprecedented new mechanism in gas-phase dissociation of protein oligomers whereby a tetramer complex dissociates into two dimers. These data add to the current debate whether gas-phase structures of protein complexes do retain some of the structural features of the corresponding species in solution. The presented low-cost modifications on a Q-TOF 1 instrument are of interest to everyone working in the fields of macromolecular mass spectrometry and more generic structural biology.

In recent years, electrospray ionization (ESI) mass spectrometry has become an increasingly important method not only to analyze peptides in proteomics<sup>1,2</sup> but also to study proteins and protein complexes of increasing size and complexity in structural biology.<sup>3,4</sup> The analysis of proteins and protein complexes by mass spectrometry (macromolecular mass spectrometry) has become

possible because of the development of a relatively gentle ionization procedure, ESI, which retains noncovalent interactions.<sup>5</sup> In the ESI process, a transition of the protein in the solution phase to highly charged droplets and, finally, to protein ions in the gas phase takes place by a combination of collision-induced and thermal desolvation. When the ESI process is carried out on folded proteins using aqueous buffers, that is, near physiological conditions, series of relatively lowly charged protein ions are produced. The mass-to-charge ( $m/z$ ) ratios of these proteins can well be over 10 000, and therefore, time-of-flight (TOF) analyzers with orthogonal injection are the most commonly used analyzers in the field of macromolecular mass spectrometry.

The mass analysis of larger proteins and protein complexes is not a routine technique, since a careful optimization of the operating conditions is always required. Despite the theoretically unlimited mass range of TOF analyzers, most instruments have detection problems when the  $m/z$  values exceed 4000. We and others have shown that a pressure increase in the first and second vacuum chamber of the mass spectrometer is an absolute requirement for the analysis of large proteins.<sup>6–10</sup> The increased pressure leads to collisional cooling and focusing of large ions in the ion guides and, therefore, improved transmission through the ion guides and the TOF.<sup>9</sup>

For the analysis of a single protein, mass measurement is often sufficient and can identify, for example, protein modifications and the oligomerization state. However, when more complex biomolecules, such as protein complexes or protein-DNA complexes, are analyzed, mass measurement alone is insufficient to delineate all

\* Corresponding author. Phone: +31302536797. Fax: +31302518219. E-mail: ajrheck@chem.uu.nl.

<sup>†</sup> Utrecht University.

<sup>‡</sup> Wageningen University.

<sup>§</sup> MS Horizons.

(1) Ong, S. E.; Mann, M. *Nat. Chem. Biol.* **2005**, *1*, 252–262.

(2) Yates, J. R.; Gilchrist, A.; Howell, K. E.; Bergeron, J. J. M. *Nat. Rev. Mol. Cell Biol.* **2005**, *6*, 702–714.

(3) van den Heuvel, R. H.; Heck, A. J. *Curr. Opin. Chem. Biol.* **2004**, *8*, 519–526.

(4) Benesch, J. L.; Robinson, C. V. *Curr. Opin. Struct. Biol.* **2006**, *16*, 245–251.

(5) Fenn, J. B.; Mann, M.; Meng, C. K.; Wong, S. F.; Whitehouse, C. M. *Science* **1989**, *246*, 64–71.

(6) Sanglier, S.; Leize, E.; Van Dorsselaer, A.; Zal, F. *J. Am. Soc. Mass Spectrom.* **2003**, *14*, 419–429.

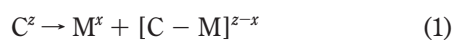
(7) Schmidt, A.; Bahr, U.; Karas, M. *Anal. Chem.* **2001**, *73*, 6040–6046.

(8) Tahallah, N.; Pinkse, M.; Maier, C. S.; Heck, A. J. *Rapid Commun. Mass Spectrom.* **2001**, *15*, 596–601.

(9) Chernushevich, I. V.; Thomson, B. A. *Anal. Chem.* **2004**, *76*, 1754–1760.

(10) Krutchinsky, A. N.; Chernushevich, I. V.; Spicer, V. L.; Ens, W.; Standing, K. G. *J. Am. Soc. Mass Spectrom.* **1998**, *9*, 569–579.

possible combinations of proteins and their ligands. An additional problem for mass spectrometry of very large (heterogeneous) complexes is the high number of charges these complexes attain and the potential overlap of ions from different species present in the sample, which makes the mass spectra very complicated. For these more complex samples, tandem mass spectrometry can be used to dissect complexes in the gas phase in a sequential fashion to identify the building blocks and potentially also complex topology, quaternary structure, and stability.<sup>11</sup> In tandem mass spectrometry experiments, an ion is selected on the basis of the  $m/z$  value in the first quadrupole mass analyzer, after which the selected ion is dissociated in a gas-filled collision cell. The subsequent TOF analyzer then allows the detection of the product ions. Early studies with hemoglobin showed that activation of the noncovalent oligomeric complex in the mass spectrometer results in the dissociation of one monomer, which carried more charges than expected on the basis of the monomer molecular mass.<sup>12</sup> Further studies have shown that the asymmetric separation of mass and charge is a common phenomenon for gas-phase dissociation of protein complexes (for recent reviews on this topic, see refs 13 and 14). The common pathway of gas-phase, collision-induced, protein complex dissociation inside the mass spectrometer can be described as follows



where C is the protein complex, M is dissociated monomeric subunit,  $z$  is the number of charges of the complex, and  $x$  is the number of charges carried by the dissociated monomeric subunit.

Tandem mass spectrometry of large protein complexes is a relatively new field in macromolecular mass spectrometry. This is due to the fact that most commercial quadrupoles can transmit ions to a certain limit, which is dependent on the RF amplitude, frequency, and diameter of the rod assembly. The transmission limit ( $M_{\max}$ ) is given by

$$M_{\max} = 7 \times 10^6 V_m / f^2 r_0^2 \quad (2)$$

with  $V_m \cos(2\pi ft)$  as the RF voltage applied between the rods ( $2V_m$  is the peak-to-peak amplitude;  $f$ , the frequency; and  $t$ , the time) and  $r_0$  as the inner radius between the rods. A standard first generation Q-TOF 1 (Micromass) operates at a frequency of 832 kHz, setting the transmission limit to  $m/z$  4190. By replacing the standard RF generator with a RF generator that operates at a lower frequency, the upper transmission limit can, at the cost of mass resolution, be extended.<sup>15,16</sup> Because the quadrupole is used only

as a mass filter to isolate ions for tandem mass spectrometry and the TOF analyzer is used to mass analyze the product ion spectrum, the instrument performance is not compromised significantly.

In this project, we have modified and optimized a first generation Q-TOF 1 instrument for macromolecular tandem mass spectrometry. As pointed out above, two critical factors had to be explored: the operating pressures in the different regions of the mass spectrometer and the  $m/z$  range of the first quadrupole mass analyzer. The described low-cost modifications can be applied on all standard Q-TOF instruments. We demonstrate the potential of the instrument for macromolecular tandem mass spectrometry by studying gas-phase stabilities of chaperone complexes, vanillyl alcohol oxidase and two proteins involved in pentose metabolism, arabinose dehydrogenase and 2-keto-3-deoxyarabinonate dehydratase. The generated data allowed us to hypothesize on the relevance of these experiments in the gas phase for determining the topology and quaternary structure of protein complexes in solution.

## EXPERIMENTAL SECTION

**Chemicals and Preparation of Proteins.** The GroEL chaperonin was overexpressed in *Escherichia coli* and purified according to a previously established procedure slightly modified by the introduction of an acetone precipitation step.<sup>17,18</sup> The GroES co-chaperonin and vanillyl alcohol oxidase wild type and His61Thr mutant were each overexpressed in *E. coli* and purified as reported.<sup>19,20</sup> The vanillyl alcohol oxidase His61Thr mutant was saturated with flavin adenine dinucleotide cofactor, and an excess of cofactor was removed by elution over a Superdex 200 10/300 GL column (GE Healthcare). Arabinose dehydrogenase and 2-keto-3-deoxyarabinonate dehydratase were produced in *E. coli* and purified by a heat incubation to denature *E. coli* proteins, followed by a single affinity chromatography purification step for the arabinose dehydrogenase and two ion-exchange chromatography steps for the 2-keto-3-deoxyarabinonate dehydratase. Cesium iodide and ammonium acetate were purchased from Sigma. The nonvolatile buffers in which the proteins were purified were exchanged for aqueous 50 mM ammonium acetate, pH 6.0 or 6.8, using ultrafiltration units (Millipore, Bedford, UK) with a cutoff of 5000 Da. Final concentrations of the proteins based on their monomeric masses were 5  $\mu$ M for GroEL, 4  $\mu$ M for vanillyl alcohol oxidase, and 8  $\mu$ M for arabinose dehydrogenase and 2-keto-3-deoxyarabinonate dehydratase. For complex formation of GroEL and GroES, the two proteins were mixed, each at a concentration of 8  $\mu$ M, in the presence of 320  $\mu$ M ADP and 320  $\mu$ M magnesium acetate. An incubation time of 5 min at room temperature was used to allow complex formation.

**Mass Spectrometry.** All the mass spectrometry measurements were performed in positive ion mode. Proteins and protein complexes were introduced into the mass spectrometer by using gold-coated needles in the absence of any backpressure. The needles were made from borosilicate glass capillaries (Kwik-Fil, World Precision Instruments, Sarasota, FL) on a P-97 puller (Sutter

- (11) McCammon, M. G.; Hernandez, H.; Sobott, F.; Robinson, C. V. *J. Am. Chem. Soc.* **2004**, *126*, 5950–5951.
- (12) Light-Wahl, K. J.; Schwartz, B. L.; Smith, R. D. *J. Am. Chem. Soc.* **1994**, *116*, 5271–5278.
- (13) Heck, A. J.; Van Den Heuvel, R. H. *Mass Spectrom. Rev.* **2004**, *23*, 368–389.
- (14) Sobott, F.; McCammon, M. G.; Hernandez, H.; Robinson, C. V. *Philos. Transact. R. Soc. London, Ser. A* **2005**, *363*, 379–389; discussion 389–391.
- (15) Sobott, F.; Hernandez, H.; McCammon, M. G.; Tito, M. A.; Robinson, C. V. *Anal. Chem.* **2002**, *74*, 1402–1407.
- (16) Loo, J. A.; Berhane, B.; Kaddis, C. S.; Wooding, K. M.; Xie, Y. M.; Kaufman, S. L.; Chernushevich, I. V. *J. Am. Soc. Mass Spectrom.* **2005**, *16*, 998–1008.

- (17) Voziyan, P. A.; Fisher, M. T. *Protein Sci.* **2000**, *9*, 2405–2412.
- (18) Quaiter-Randall, E.; Joachimiak, A. *Methods Mol. Biol.* **2000**, *140*, 29–39.
- (19) Quaiter-Randall, E.; Joachimiak, A. *Methods Mol. Biol.* **2000**, *140*, 41–49.
- (20) van den Heuvel, R. H.; Fraaije, M. W.; Mattevi, A.; van Berkel, W. J. *J. Biol. Chem.* **2000**, *275*, 14799–14808.

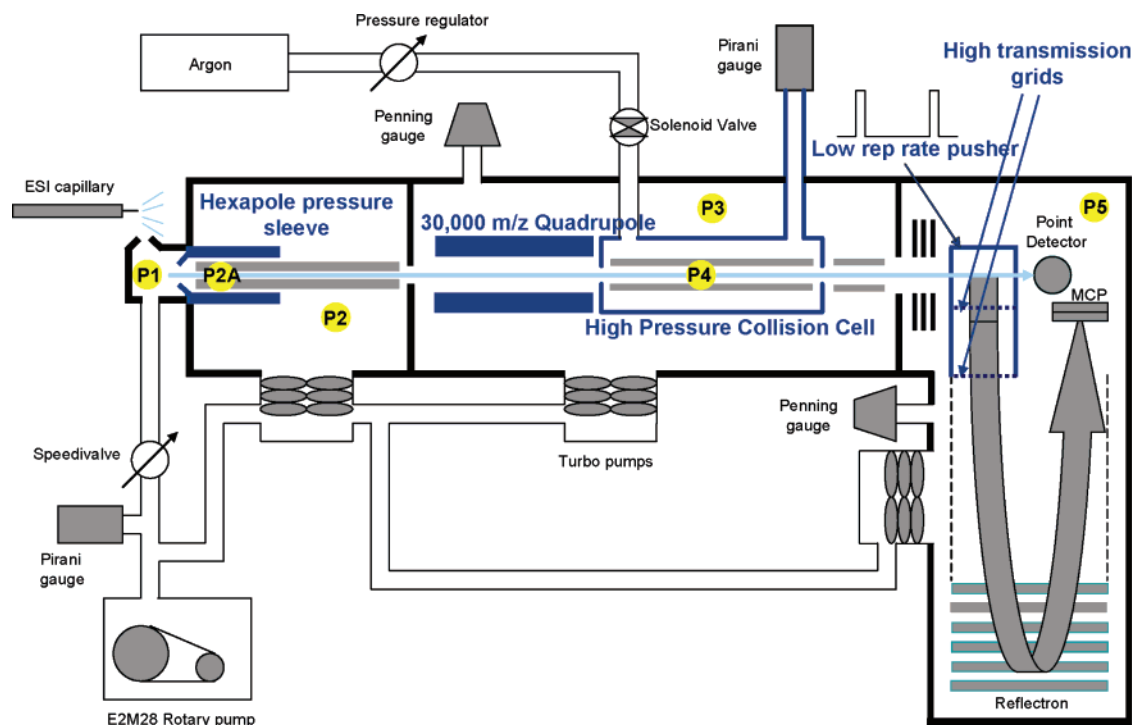


**Figure 1.** Schematic layout of the modified first generation Q-TOF 1 instrument (Micromass, U.K.). For details of modifications see the Experimental Section. Items in dark blue are modifications relative to the standard Q-TOF 1 configuration.

Instruments, Novato, CA) and coated with a thin gold layer by using an Edwards Scancoat (Edwards Laboratories, Milpitas, CA) six Pirani 501 sputter coater. All the mass spectra were calibrated using cesium iodide (5–25 mg/mL) in 50% (v/v) 2-propanol. The instrument that was modified was a first generation Q-TOF 1 instrument (Micromass, Manchester, UK) equipped with a Z-spray source. All modifications are schematically presented in Figure 1 and explained and discussed in this section. With the exception of the adjustment of some settings to allow for the analysis and registration of high- $m/z$  ions, the computer hardware and software was not modified. MassLynx version 3.5 (Micromass) was used for the data analysis.

Electrospray ions were produced at atmospheric pressure, after which the partly solvated ions were introduced into the first vacuum stage (P1) of the mass spectrometer through a sample cone with an orifice of 400  $\mu\text{m}$ . The pressure in P1 was increased by reducing the pumping efficiency of the rotary pump to 10 mbar (unless stated otherwise in the text). The molecular beam of charged ions that evolves behind the sample cone was then extracted orthogonally through an extractor cone with an orifice of 1 mm into the second pumping stage (P2;  $4 \times 10^{-3}$  mbar). The cone voltage used was dependent on the type of protein complex and varied between 75 and 150 V. The ions that entered the second pumping stage (P2) were focused by a hexapole ion guide. Around the first part of the hexapole, a flow-restricting sleeve in the form of a metal tube (25 mm i.d., 100 mm long) was installed to increase the pressure locally (P2A; estimated average pressure  $8 \times 10^{-3}$  mbar). In a slightly different form, this modification has been reported by Chernushevich and Thomson.<sup>9</sup> The third vacuum chamber (P3;  $6.7 \times 10^{-4}$  mbar) contains a quadrupole, a separate collision cell, and a transport hexapole lens. The standard RF generator in the Q-TOF was replaced by a generator with a frequency of operation of 300 kHz.<sup>21</sup> This sets the theoretical accessible

transmission limit for a selected ion to 30 000  $m/z$  according to eq 2. When acquiring TOF mass spectra, the quadrupole operates in RF-only mode as a broad-band mass filter. However, in the tandem mass spectrometry mode, the quadrupole transmits only ions in a narrow  $m/z$  window around a set  $m/z$ , thus operating as a narrow-band mass filter. Ions are then transferred to the hexapole collision cell, which was modified such that the argon gas pressure can be increased. To measure protein complexes, we used a cylinder head pressure of 2.0 bar (unless stated otherwise in the text) admitted to the collision cell via a needle leak valve with a 100- $\mu\text{m}$  capillary with a length of 1.25 m leading to a pressure of  $1.5 \times 10^{-2}$  mbar in the collision cell (P4). If the gas pressure is too low, ions can be transferred to the TOF analyzer without dissociation. Both the entrance and exit orifices of the collision cell are 2 mm. After activation in the collision cell, the ions are transferred to the TOF vacuum chamber (P5;  $2 \times 10^{-6}$  mbar). A multicomponent ion lens focuses the ions, and two of the meshes were changed from 1000 to 200 lines/inch for a 3-fold enhancement of the sensitivity. When the ions arrived in the pusher region, they were pulsed orthogonally for TOF analysis. The TOF repetition rate was decreased to 410  $\mu\text{s}$  to increase the maximum attainable  $m/z$ , which theoretically could be 58 000.

## RESULTS AND DISCUSSION

**Efficient Transmission of GroEL Ions in a Modified Q-TOF 1 Instrument.** The custom-modified Q-TOF 1 instrument was designed to analyze multiple charged ions of large protein complexes. To analyze these ions by mass spectrometry, several conditions had to be optimized. Insufficient axial cooling makes ions miss the detector, whereas insufficient radial cooling results in poor transmission of ions through the different apertures in

(21) Collings, B. A.; Douglas, D. J. *Int. J. Mass Spectrom. Ion Processes* **1997**, *162*, 121–127.

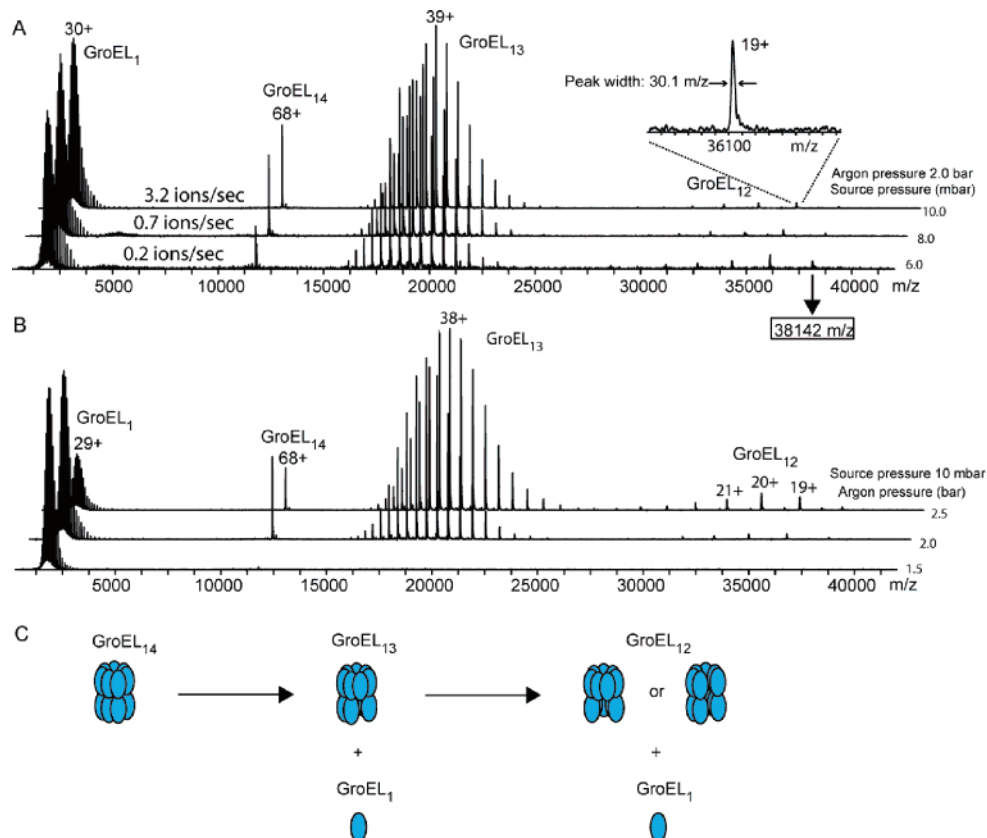


**Figure 2.** Gas-phase dissociation of GroEL<sub>14</sub> complex. Tandem mass spectrometry was performed on 0.36  $\mu$ M GroEL<sub>14</sub> in 50 mM ammonium acetate, pH 6.8. (A) Source pressure dependent tandem mass spectra of the 68<sup>+</sup> ion of GroEL<sub>14</sub> (11 780  $m/z$ ) at an acceleration voltage of 200 V. The argon pressure was kept constant at 2.0 bar (collision cell pressure of  $1.5 \times 10^{-2}$  mbar). The parent ion peak of the tetradecameric complex is almost completely dissociated into GroEL<sub>13</sub> and monomeric GroEL ions. At high collision energies (200 V), the produced tridecameric complex is, in turn, partly dissociated into GroEL<sub>12</sub> and monomeric GroEL products. These two processes take place in sequential order. The inset shows the fwhm of the 19<sup>+</sup> GroEL<sub>12</sub> ion at  $m/z$  38 142. (B) Argon-gas-pressure-dependent tandem mass spectra of the 68<sup>+</sup> ion of GroEL<sub>14</sub> at an acceleration voltage of 200 V. The source pressure was kept constant at 10 mbar. (C) Schematic representation of gas-phase dissociation process of the GroEL<sub>14</sub> oligomer. GroEL monomers are sequentially ejected from the intact GroEL<sub>14</sub> and GroEL<sub>13</sub> complexes.

the mass spectrometer. With the aim to optimize precursor and product ion transmission, we analyzed GroEL<sub>14</sub> oligomer (801 kDa) under different conditions. We selected the 68<sup>+</sup> GroEL<sub>14</sub> ion ( $\sim 11\,800\,m/z$ ) in the quadrupole analyzer and accelerated the ions in the argon-filled collision cell with 200 V. This yielded tandem mass spectra with product ions in the  $m/z$  range from 2000 up to 40 000, which allowed us to optimize the Q-TOF 1 instrument in a broad  $m/z$  range. The low- $m/z$  ions around 2000 represented ejected monomeric GroEL ions, and the high- $m/z$  ions in the range 15 000–40 000, the stripped oligomers. The in-depth analysis of the gas-phase dissociation pattern of GroEL<sub>14</sub> oligomer is described in the next section.

First, we acquired tandem mass spectra at different source pressures (P1) between the sample and extraction cone by tuning the speedivalve.<sup>6–10</sup> The pressures at the other stages in the mass spectrometer were kept constant. Reducing the pumping efficiency of the rotary pump up to 10 mbar clearly led to an enhanced detection of the GroEL ions. At a source pressure of 6.0 mbar, only 0.2 ions/s were detected after TOF analysis, whereas at a pressure of 10 mbar, 3.2 ions/s were detected (Figure 2A). Thus, the maximal achievable pressure of 10 mbar seems to be the optimal value for the transmission of the GroEL product ions. As expected, the relative abundance of the different species did not depend on the source pressure.

We also introduced a metal cylinder around the first half of the hexapole ion lens (length 100 mm) to increase the pressure locally (P2A). It was estimated that the initial pressure in the sleeve is 3-fold higher than in the rest of the hexapole and that the pressure in the sleeve decreases linearly. The experimental design was theoretically tested by simulating the ion trajectories of a GroEL<sub>14</sub> ion (801 kDa; 70<sup>+</sup> ion) within the modified hexapole ion guide using a method similar to that of Chenushevich and Thomson (Figure 3).<sup>9</sup> This figure clearly shows that to avoid significant GroEL<sub>14</sub> ion losses on the different apertures, a combination of an increased pressure of  $4 \times 10^{-3}$  mbar in the hexapole vacuum chamber (P2) and a locally increased pressure around the first part of the hexapole lens were required (P2A).

In addition to the source and hexapole ion bridge pressure conditions, the argon cylinder head pressure and, thus, the collision cell pressure influence the transport of the ions to the transport hexapole and the TOF analyzer.<sup>15</sup> We varied the argon head pressure to optimize the gas-phase dissociation of the GroEL<sub>14</sub> oligomer (Figure 2B). The pressures in the other stages in the instrument were kept constant, and the source pressure was set at 10 mbar. The tandem mass spectra clearly show the influence of the argon pressure on the transmission of the high- and low- $m/z$  ions to the transport hexapole lens and the TOF analyzer (Figure 2B). At a relatively low argon pressure of 1.5



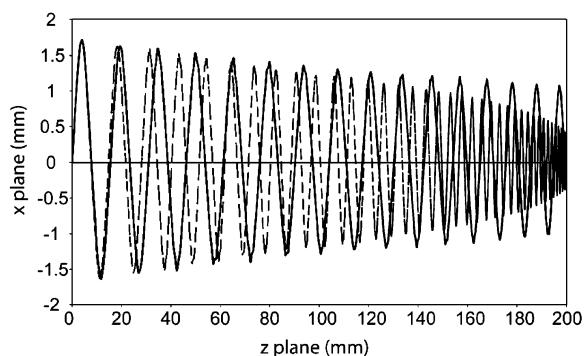


**Figure 3.** Simulated GroEL ion trajectories. Simulated were the  $68^+$  GroEL ion trajectories in the hexapole ion lens in the  $xz$  plane, at gas pressures of  $4 \times 10^{-3}$  mbar (solid line) and  $4 \times 10^{-3}$  mbar, including the metal sleeve around the first half of the hexapole lens (dashed line). The pressure is estimated to be, on average, 2-fold higher than in the remaining of the hexapole ion bridge. The ion has an initial velocity of 185 m/s and is aligned  $30^\circ$  off the optic axis.

bar ( $8 \times 10^{-3}$  mbar in the collision cell), only the low- $m/z$  ions were efficiently transmitted. At this pressure, the precursor  $68^+$  GroEL ion (11 780  $m/z$ ) had a very low intensity in the tandem mass spectrum. When the pressure was increased to 2.0 bar (collision cell pressure  $1.5 \times 10^{-2}$  mbar), the precursor GroEL ion and the high- $m/z$  product ions became more abundant in the mass spectrum. Upon further increasing the argon pressure to 2.5 bar ( $2 \times 10^{-2}$  mbar in the collision cell), the abundance of the low- $m/z$  ions decreased, and the abundance of the high- $m/z$  ions increased. Because the precursor ion dissociated in monomers (low  $m/z$  values) and stripped oligomers (high  $m/z$  values), the abundance of these two species will be identical. Thus, the low- $m/z$  product ions representing monomeric GroEL and the high- $m/z$  ions representing stripped oligomers should have similar intensities in the tandem mass spectra. This prerequisite was best fulfilled at an argon pressure of 2.0 bar, and therefore, this argon pressure was used to analyze the gas-phase stability of GroEL chaperonins.

**Gas-Phase Dissociation of GroEL Oligomers.** Molecular chaperones are essential for correct folding of a variety of different proteins. The GroEL<sub>14</sub>–GroES<sub>7</sub> complex from *Escherichia coli* is one of the best-studied chaperone machines that assists in the folding of  $\sim 10\%$  of all newly synthesized polypeptides.<sup>22</sup> GroEL<sub>14</sub> (801 kDa) is composed of two heptameric rings stacked back-to-back, each containing a distinct large central cavity. The heptameric co-chaperonin GroES<sub>7</sub> (73 kDa) binds, in the presence of ADP or ATP and  $Mg^{2+}$ , on top of one of the GroEL<sub>14</sub> rings, and an enclosed cavity is formed. Previous gas-phase dissociation experiments on unliganded GroEL<sub>14</sub> using a Q-TOF 2 instrument have demonstrated that a highly charged GroEL subunit dissociates from the oligomer upon increasing the collision energy.<sup>23,24</sup> Here, we have studied the gas-phase stability of the GroEL<sub>14</sub> oligomer and the GroEL<sub>14</sub>–GroES<sub>7</sub> chaperonin complex using the custom-modified Q-TOF 1 instrument. The mechanism of gas-

phase dissociation of subunits from protein complexes is a poorly understood process; however, it is generally accepted that multicomponent protein complexes dissociate via a similar pathway, that is, expulsion of the smallest monomeric subunit (<sup>13</sup> and references therein). The studies on this topic suggest that asymmetric charge distribution may depend on internal energy, protein complex gas-phase conformation, charge state of the ion, and the conformational stability of individual subunits. The asymmetric charge partitioning probably proceeds via unfolding of the leaving protein subunit in a dissociative transition state. This requires a large amount of energy, but it is thought to be entropically favorable.

The GroEL oligomer (GroEL<sub>14</sub>) was present in 50 mM ammonium acetate, pH 6.8, and the capillary and cone voltages were typically set at 1400 and 150 V, respectively. First, the generated GroEL<sub>14</sub> ions were accelerated, without ion selection, into the argon-filled linear hexapole collision cell and analyzed in the TOF analyzer. Upon increasing the collision energy, the mass spectrum of GroEL<sub>14</sub> showed the loss of buffer molecules and ions from GroEL<sub>14</sub>, which resulted in very narrow peaks, allowing accurate mass determination. Because the full width at half-maximum (fwhm) of the  $68^+$  ion of GroEL<sub>14</sub> was 11.8  $m/z$ , the maximum mass error was 800 Da (0.01% of the chaperonin mass). The difference between the determined molecular mass (800 977 Da) and the mass calculated from the primary sequence (800 758 Da) was only 219 Da, thus well within the calculated maximum mass error. Second, the  $68^+$  ion of GroEL<sub>14</sub> at an  $m/z$  value of 11 780 was selected in the quadrupole analyzer and accelerated in the gas-filled collision cell. At relatively low acceleration voltages ( $<150$  V), we observed primarily some decharging of the intact tetradecameric ions. This phenomenon is likely caused by the stripping of positively charged buffer ions attached to the protein surface.<sup>23</sup> Upon increasing the acceleration voltage to 150 V, a highly charged monomeric GroEL subunit was ejected from the tetradecameric complex (Figure 2A). When the collision energy was further increased to 190 V, we observed the subsequent dissociation of a second GroEL monomer from the tridecameric complex (GroEL<sub>13</sub>). This resulted in the formation of dodecameric GroEL (GroEL<sub>12</sub>) product ions and GroEL monomer ions with a lower charge state as compared to the monomer dissociated from the tetradecamer. The GroEL<sub>12</sub> product ions became even more abundant at an acceleration voltage of 200 V (Figure 3A).

Although the absolute number of charges the GroEL monomers obtained in the second dissociation event was lower, the percentage of charges that was taken up by the first and second GroEL monomer was similar. Upon dissociation of the first GroEL monomer, which accounts for 7% of the tetradecameric complex mass, it obtained 41% of the number of charges, whereas upon dissociation of the second GroEL monomer, which accounts for 9% of the tridecameric complex mass, it obtained 47% of the number of charges. As a consequence of the monomers' taking such a large number of charges, the GroEL<sub>12</sub> had an average charge state of only  $19^+$ . Therefore, these ions appeared at very high  $m/z$  values between  $\sim 28\,600$  ( $24^+$ ) and  $\sim 38\,150$  ( $18^+$ ). Even at these high values, our Q-TOF 1 mass spectrometer allowed extremely accurate mass determinations. The predicted mass of the GroEL<sub>12</sub> complex is 686 364 Da, whereas we determined a mass of 686 461 Da. This is an increase of 97 Da and only 0.01%

(22) Houry, W. A.; Frishman, D.; Eckerskorn, C.; Lottspeich, F.; Hartl, F. U. *Nature* **1999**, *402*, 147–154.

(23) Sobott, F.; Robinson, C. V. *Int. J. Mass Spectrom.* **2004**, *236*, 25–32.

(24) van Duijn, E.; Bakkes, P. J.; Heeren, R. M.; van den Heuvel, R. H.; van Heerikhuizen, H.; van der Vies, S. M.; Heck, A. J. *Nat. Methods* **2005**, *2*, 371–376.

of the total mass. This mass difference lies well within the mass error of  $\sim 572$  Da calculated from the fwhm of the  $19^+$  ion of GroEL<sub>12</sub> (Figure 2A, inset).

**Gas-Phase Stability of GroEL–GroES Chaperonin Complexes.** We continued our studies with the analysis of the functional GroEL<sub>14</sub>–GroES<sub>7</sub> chaperonin machine in 50 mM ammonium acetate, pH 6.8, and excess ADP and Mg<sup>2+</sup> ions. The chaperonin machine consists of 21 protein subunits and has a mass of  $\sim 875$  kDa. We selected the  $68^+$  charge state ion of the intact complex at  $m/z$  12 800 and gradually increased the acceleration voltage in the gas-filled collision cell. In line with solution-phase dissociation, it may be expected that increasing the collision energy would induce dissociation of the heptameric GroES<sub>7</sub> from the GroEL<sub>14</sub> oligomer. However, at a collision energy of 100 V, we observed the gas-phase dissociation of highly charged monomeric GroES (GroES) product ion around  $m/z$  1100 and the subsequent formation of GroEL<sub>14</sub>–GroES<sub>6</sub> ions around  $m/z$  14 500 (Figure 4A). The relative abundance of these GroEL<sub>14</sub>–GroES<sub>6</sub> ions increased up to a collision energy of 130 V, after which their numbers started to decrease. This was caused by the dissociation of a second GroES monomer from GroEL<sub>14</sub>–GroES<sub>6</sub>, resulting in the formation of highly charged GroES ions and lowly charged GroEL<sub>14</sub>–GroES<sub>5</sub> ions around  $m/z$  1100 and 16 000, respectively. Even a third highly charged GroES monomer could be expelled from the GroEL<sub>14</sub>–GroES<sub>5</sub> complex by increasing the collision energy to 150 V, with the subsequent formation of GroEL<sub>14</sub>–GroES<sub>4</sub> ions. Intriguingly, only at very high collision energies of 190–200 V did we observe the dissociation of one GroEL subunit from GroEL<sub>14</sub>–GroES<sub>7</sub>, resulting in the formation of GroEL and GroEL<sub>13</sub>–GroES<sub>7</sub> products ions around  $m/z$  1850 and 28 000, respectively (Figure 4B, C). Mass determination of the ejected GroEL monomer clearly showed that ADP (427 Da) was not present on these highly charged monomeric fragments (determined mass 57 261 Da vs predicted mass 57 197 Da).

At first, the results with GroEL<sub>14</sub> and GroEL<sub>14</sub>–GroES<sub>7</sub> may indicate that it is more difficult to dissociate a GroEL monomer from the complete chaperonin GroEL<sub>14</sub>–GroES<sub>7</sub> complex than from free GroEL because a higher collision voltage is required (190 V vs 150 V). However, to draw conclusions about energy dependence of gas-phase dissociation data for different noncovalent complexes, it is not correct to use these collision voltage values directly. Instead, the center-of-mass collision energy needs to be calculated. The center-of-mass collision energy is the maximum amount of kinetic energy that can be converted into internal energy upon collision activation under single collision conditions<sup>25</sup> and may be estimated by

$$E_{\text{com}} = E_{\text{lab}} m_{\text{target}} / (m_{\text{protein}} + m_{\text{target}}) \quad (3)$$

where  $E_{\text{lab}}$  (eV) is the ion kinetic energy in the laboratory frame of reference,  $m_{\text{target}}$  is 40 Da (the mass of the argon collision partner) and  $m_{\text{protein}}$  is  $\sim 875$  kDa. Because the dissociation process inside the collision cell of the Q-TOF is a multiple collision event, the center-of-mass calculation is not accurate, especially for larger complexes. Nevertheless, the current approach allows, to some extent, semiquantitative comparisons. If we calculate the  $E_{\text{com}}$

values at which free GroEL<sub>14</sub> and GroEL<sub>14</sub>–GroES<sub>7</sub> start to dissociate the first GroEL monomer, these values are very similar (0.51 and 0.54 eV, respectively) and are expected to be within the  $E_{\text{com}}$  error. These values, thus, strongly suggest that it is not more complicated for the GroEL<sub>14</sub>–GroES<sub>7</sub> complex to eject one monomer than it is for the free GroEL<sub>14</sub> complex. Therefore, these calculations indicate that the formation of the functional GroEL–GroES chaperonin from GroEL<sub>14</sub> hardly influences the gas-phase stability of the two heptameric rings composed of GroEL subunits.

**Flavin Binding Mode Does Not Influence Gas-Phase Stability of Vanillyl Alcohol Oxidase.** Vanillyl alcohol oxidase is a flavoprotein containing a covalently bound FAD cofactor. The enzyme catalyzes the oxidation of a wide range of substituted phenolic compounds.<sup>26</sup> A few years ago, we reported on the oligomeric state of the protein in solution and the influence of the binding FAD cofactor on the oligomeric state.<sup>27</sup> Our data showed that the oligomeric state of vanillyl alcohol oxidase is actually an equilibrium between two states, that is, a dimeric and octameric state whereby the equilibrium is directed far toward the octameric species with a mass of 509 kDa. Macromolecular mass spectrometry and size-exclusion chromatography analysis showed that the equilibrium of the apo-His61Thr mutant oxidase, which does not contain the covalently bound FAD, is shifted toward the dimeric form,<sup>28</sup> suggesting that the covalently attached FAD molecule is important to shift the equilibrium toward the biologically active form of the enzyme. Here we report on the gas-phase stability of the wild-type vanillyl alcohol oxidase and the holo-His61Thr mutant using tandem mass spectrometry.

First, the dissociation pattern of vanillyl alcohol oxidase in 50 mM ammonium acetate, pH 6.8, was determined. As was observed before, the mass spectrum of intact vanillyl alcohol oxidase clearly showed the dimeric and octameric species (data not shown). Tandem mass spectrometry on the isolated  $52^+$  ion of the octamer clearly showed dissociation of a highly charged monomer around  $m/z$  2300, with the subsequent formation of a lowly charged heptamer around  $m/z$  18 500 (Figure 5A). This is in sharp contrast to the solution phase in which the octamer is in equilibrium with the dimer, gas-phase dissociation showed only ejection of a monomeric species. As may be expected from the covalently bound flavin cofactor, all heptamers and dissociated monomers were fully saturated with the flavin. For subunit dissociation, a minimum acceleration voltage of 150 V (0.61 eV) was required and even at the highest collision energy significant amounts of octameric species remained present. These results clearly showed that the vanillyl alcohol oxidase subunits form a very stable octamer in the gas phase.

These experiments were repeated for the FAD saturated holo-His61Thr mutant in 50 mM ammonium acetate buffer, pH 6.8. The measured mass of 509 150 Da was in good agreement with the expected mass including eight noncovalently bound flavin molecules (509 224 Da), strongly indicating that the enzyme was fully saturated with the flavin cofactor. At relatively low collision energies ( $<100$  V), tandem mass spectrometry on the isolated

(25) Jorgensen, T. J. D.; Delforge, D.; Remacle, J.; Bojesen, G.; Roepstorff, P. *Int. J. Mass Spectrom.* **1999**, *188*, 63–85.

(26) Fraaije, M. W.; Veeger, C.; van Berkel, W. J. *Eur. J. Biochem.* **1995**, *234*, 271–277.

(27) van Berkel, W. J.; van den Heuvel, R. H.; Versluis, C.; Heck, A. J. *Protein Sci.* **2000**, *9*, 435–439.

(28) Tahallah, N.; Van Den Heuvel, R. H.; Van Den Berg, W. A.; Maier, C. S.; Van Berkel, W. J.; Heck, A. J. *J. Biol. Chem.* **2002**, *277*, 36425–36432.

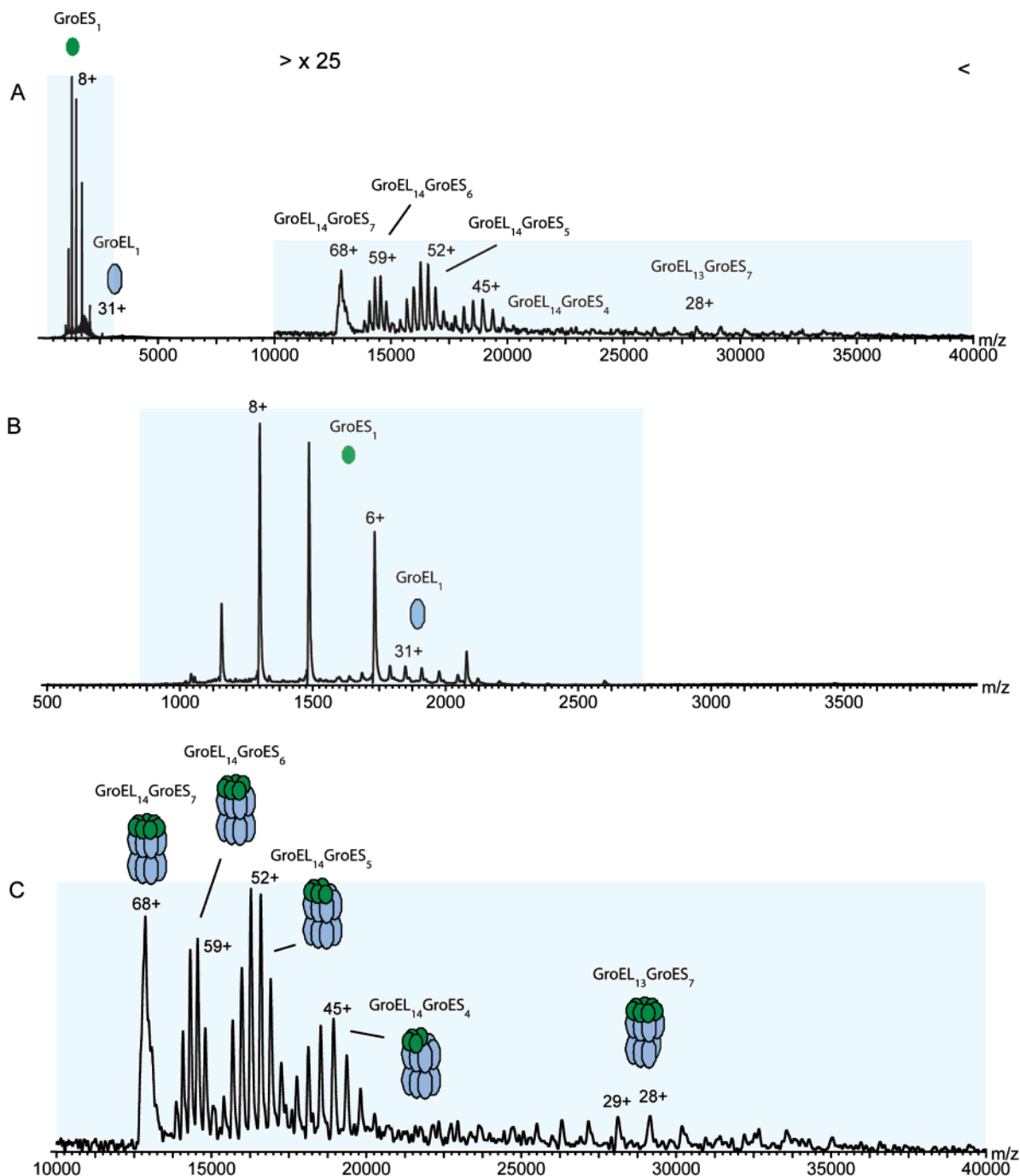


**Figure 4.** Gas-phase dissociation of GroEL<sub>14</sub>-GroES<sub>7</sub> chaperonin. Tandem mass spectrometry was performed on 0.5  $\mu$ M GroEL<sub>14</sub>-GroES<sub>7</sub> in 50 mM ammonium acetate, pH 6.8. (A) Tandem mass spectrum of the  $68^+$  ion of the GroEL<sub>14</sub>-GroES<sub>7</sub> complex at an acceleration voltage of 200 V. The gray areas are enlarged in B and C. (B) Tandem mass spectrum of the  $68^+$  ion at an acceleration voltage of 200 V in the  $m/z$  region 500–4000. Indicated are dissociated GroES subunits and one GroEL subunit. (C) Tandem mass spectrum of the  $68^+$  ion at a collision voltage of 200 V in the  $m/z$  region 10 000–40 000. Indicated is the precursor GroEL<sub>14</sub>-GroES<sub>7</sub> ion ( $68^+$ ), GroEL<sub>14</sub>-GroES<sub>6</sub>, GroEL<sub>14</sub>-GroES<sub>5</sub>, and GroEL<sub>13</sub>-GroES<sub>7</sub>.

$52^+$  ion of the holo-His61Thr octamer initially showed partial loss of up to three neutral flavin molecules. Due to the poor desolvation at low acceleration voltages, we can not, however, exclude that a small part of the protein was not fully saturated with the cofactor. This incomplete desolvation is a common phenomenon for large protein complexes.<sup>23,24</sup> Surprisingly, when the collision energy was further increased to 150 V, no further dissociation of flavin molecules was observed (Figure 5B, inset). Around a collision energy of 150 V (0.61 eV), we observed dissociation of highly

charged monomeric His61Thr ions around  $m/z$  2200 (Figure 5B). The determined mass of the dissociated monomer (62 805 Da) was in good agreement with the calculated mass based on the primary sequence of His61Thr in the absence of the flavin cofactor (62 868 Da). Thus, the dissociated monomers did not contain the noncovalently bound flavin molecule. The stripped heptameric His61Thr ions were detected around  $m/z$  17 000 and showed also losses of flavin molecules. Flavin molecular ions could, indeed, be observed in the low- $m/z$  region (data not shown). Dissociation



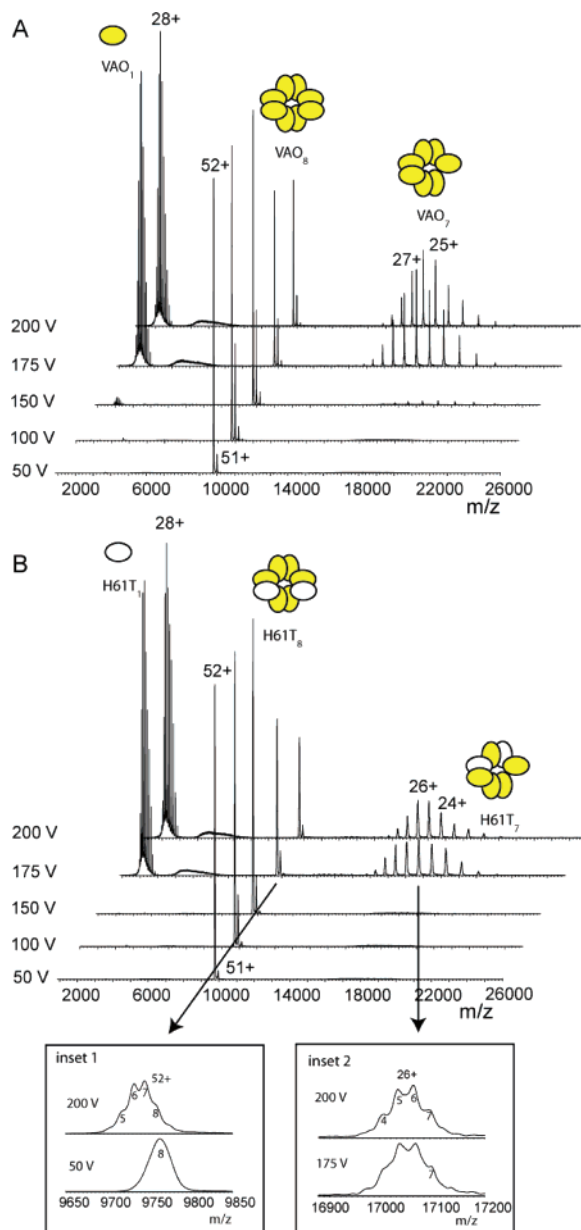


**Figure 5.** Gas-phase dissociation of vanillyl alcohol oxidase. Tandem mass spectrometry was performed on 4  $\mu$ M vanillyl alcohol oxidase (VAO) and His61Thr mutant in 50 mM ammonium acetate, pH 6.8. (A) Tandem mass spectra of vanillyl alcohol oxidase at collision cell energies ranging from 50 to 200 V after selection of the 52<sup>+</sup> octameric ion and (B) tandem mass spectra of His61Thr mutant at collision cell energies ranging from 50 to 200 V after selection of the 52<sup>+</sup> octameric ion. Inset 1 shows the 52<sup>+</sup> precursor ion of the His61Thr mutant at 50 and 200 V, and inset 2 shows the 26<sup>+</sup> heptamer ion of His61Thr mutant at 175 and 200 V.

of an apo-His61Thr subunit from the octameric precursor did not induce further release of flavin molecules. Upon further increasing the collision energy from 150 to 200 V, no subsequent dissociation of a second His61Thr monomer was observed.

The tandem mass spectrometry data, thus, clearly showed that the gas-phase stabilities of wild type and mutant vanillyl alcohol oxidase are very similar. Thus, the presence of a covalent flavin molecule bound to the enzyme does not enhance the gas-phase stability of vanillyl alcohol oxidase. The data also indicate that the stripped heptameric His61Thr ions still have some tertiary

and quaternary structure because the noncovalently bound flavin molecules did not dissociate completely from the oligomer.

**Unusual Gas-Phase Dissociation of Tetrameric Protein Complexes.** At first glance, the functionally related 2-keto-3-deoxyarabinonate dehydratase and arabinose dehydrogenase from the hyperthermophilic archaeon *Sulfolobus solfataricus*, which are both involved in pentose metabolism, share a similar quaternary structure because they both form stable tetramers of similar size (~140 kDa). Very recently, an X-ray structure has been determined for both of these proteins. The X-ray model of 2-keto-3-deoxyarabinonate dehydratase revealed that the protein is a donut-shaped tetramer of two dimers in which the dimers have a restricted number of contacts and in which each monomer is stabilized by intersubunit contacts with two other monomers. Thus, in this topology, each monomer contacts only two other monomers (Figure 6). The crystallographic model of arabinose dehydrogenase showed that this enzyme is also composed of two dimers, but in here, each monomer is stabilized by extensive intersubunit interactions with three other monomers. The structural model has indicated that the protein interacts with two zinc atoms per monomer, which is in line with the zinc dependency of other medium-chain alcohol dehydrogenases.

The mass spectrum of arabinose dehydrogenase in 50 mM ammonium acetate buffer, pH 6.0, showed that the protein is present in its tetrameric form. The determined mass of 149 700 Da (including eight zinc atoms) is in close agreement with the calculated mass based on the primary sequence (149 671 Da). Isolation of the 25<sup>+</sup> ion of the tetrameric protein species and subsequent acceleration by increasing the collision energy did not result in loss of zinc atoms. At a collision energy of 160 V (0.83 eV), we observed the typical dissociation of highly charged monomeric subunits around  $m/z$  2000 and the resulting trimeric species around  $m/z$  14 000 (Figure 6A). Further increasing the collision energy to 200 V did not result in the subsequent dissociation of a second monomer, but showed some gas-phase fragmentation of the protein by the elimination of short, terminal peptide sequences.

The mass spectrum of 2-keto-3-deoxyarabinonate dehydratase measured in 50 mM ammonium acetate buffer, pH 6.0, showed that the protein exists as a tetramer with a determined mass of 132 850 Da. This mass was ~250 Da higher than the predicted mass based on the primary amino acid sequence (132 572 Da), which is likely explained by the presence of buffer and molecules within the cavity of protein oligomer. For the gas-phase stability experiments, we isolated the 27<sup>+</sup> ion of the tetramer and increased the collision energy. Surprisingly, the tetrameric precursor ion started to dissociate already at a collision energy of 50 V (0.20 eV), and the dissociation involved the formation of dimeric ions, with the ions 13<sup>+</sup> and 14<sup>+</sup> being the most abundant (Figure 6B). We were intrigued by this result because we expected, in line with the other data in this paper and literature,<sup>29,30</sup> the dissociation of a highly charged monomer from the tetramer. To the best of our knowledge, this is the first observation that gas-phase dissociation of an intact protein oligomer does not result in the preferred formation of a highly charged monomer subunit. Potentially, somewhat related, gas-phase dissociation of a peptide

(29) Versluis, C.; Heck, A. J. R. *Int. J. Mass Spectrom.* **2001**, 210/211, 637–649.

(30) Sobott, F.; McCammon, M. G.; Robinson, C. V. *Int. J. Mass Spectrom.* **2003**, 230, 193–200.

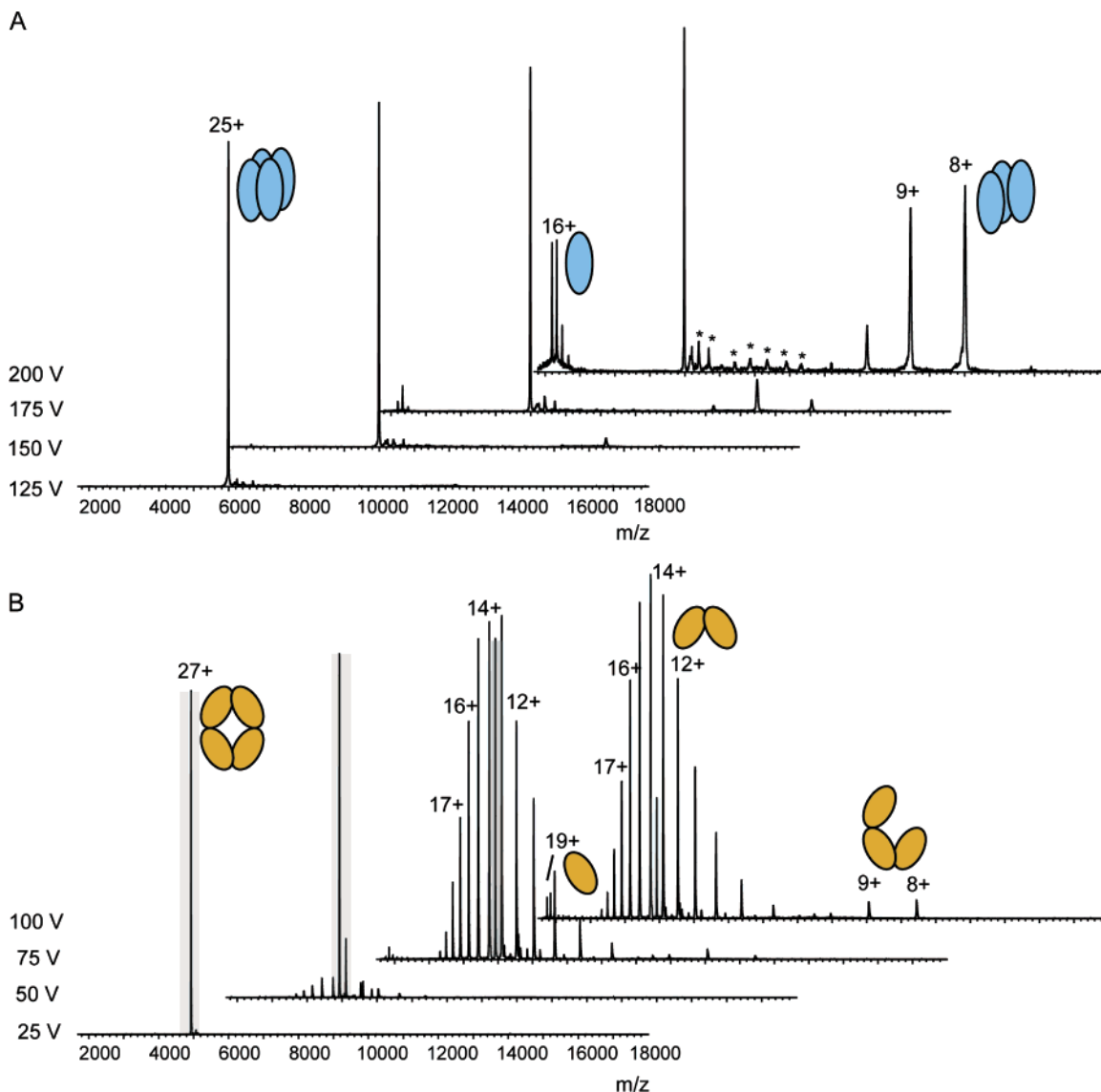


**Figure 6.** Gas-phase dissociation of arabinose dehydrogenase and 2-keto-3-deoxyarabinonate dehydratase. Tandem mass spectrometry was performed on 8  $\mu$ M of both enzymes in 50 mM ammonium acetate, pH 6.0. (A) Tandem mass spectra of arabinose dehydrogenase at acceleration voltages ranging from 50 to 200 V after selection of the 25<sup>+</sup> ion of the tetrameric species. (B) Tandem mass spectra of 2-keto-3-deoxyarabinonate dehydratase at acceleration voltages ranging from 10 to 100 V after selection of the 27<sup>+</sup> ion of the tetrameric species. The gray column indicates the precursor ion of 2-keto-3-deoxyarabinonate dehydratase. At high collision energies, some covalent fragmentation reactions took place. The stars indicate these fragments.

dimer has been reported for the gas-phase dissociation of leucine enkephalin clusters.<sup>31</sup> The 2<sup>+</sup> ion of leucine enkephalin nonamer dissociated mainly into singly charged dimeric and pentameric species. This phenomenon was explained by the exceptionally high gas-phase stability of these peptide dimers.<sup>32</sup> Due to the complexity, we simulated the tandem mass spectrum of 2-keto-3-deoxyarabinonate dehydratase using the in-house-developed software program SOMMS.<sup>33</sup> This program uses Gaussian curve fitting to simulate putative mass spectra of protein (sub)complexes within a specified charge state window. In addition, the program can simulate spectra for heterogeneous protein complexes using

bi- and multinomial distributions, and it can calculate zero-charge spectra and quantify the abundance of each component in a mixture. These simulations predicted that the ejected dimer obtained, on average, 15<sup>+</sup> charges from the total of 27<sup>+</sup> charges of the precursor tetramer. Thus, the number of charges were nearly equally divided over the two dimeric species. Upon increasing the acceleration voltage further (>85 V; 0.62 eV), highly charged monomeric ions around  $m/z$  2000 started to dissociate from the remaining precursor tetrameric protein ions. At a collision cell energy of 100 V, ~98% of the total intensity of the fragmented ions originated from the dimeric ions, whereas only ~2% originated from monomeric or trimeric ions (Figure 7). These results clearly showed that the isolated donut-shaped tetrameric protein ions preferentially dissociate into dimeric species.

The unusual dissociation pattern of 2-keto-3-deoxyarabinonate dehydratase gives rise to further discussion as to what kind of

(31) Jurchen, J. C.; Garcia, D. E.; Williams, E. R. *J. Am. Soc. Mass Spectrom.* **2003**, *14*, 1373–1386.

(32) Schnier, P. D.; Price, W. D.; Strittmatter, E. F.; Williams, E. R. *J. Am. Soc. Mass Spectrom.* **1997**, *8*, 771–780.

(33) van Breukelen, B.; Barendregt, A.; Heck, A. J.; van den Heuvel, R. H. *Rapid Commun. Mass Spectrom.* **2006**, *20*, 2490–2496.

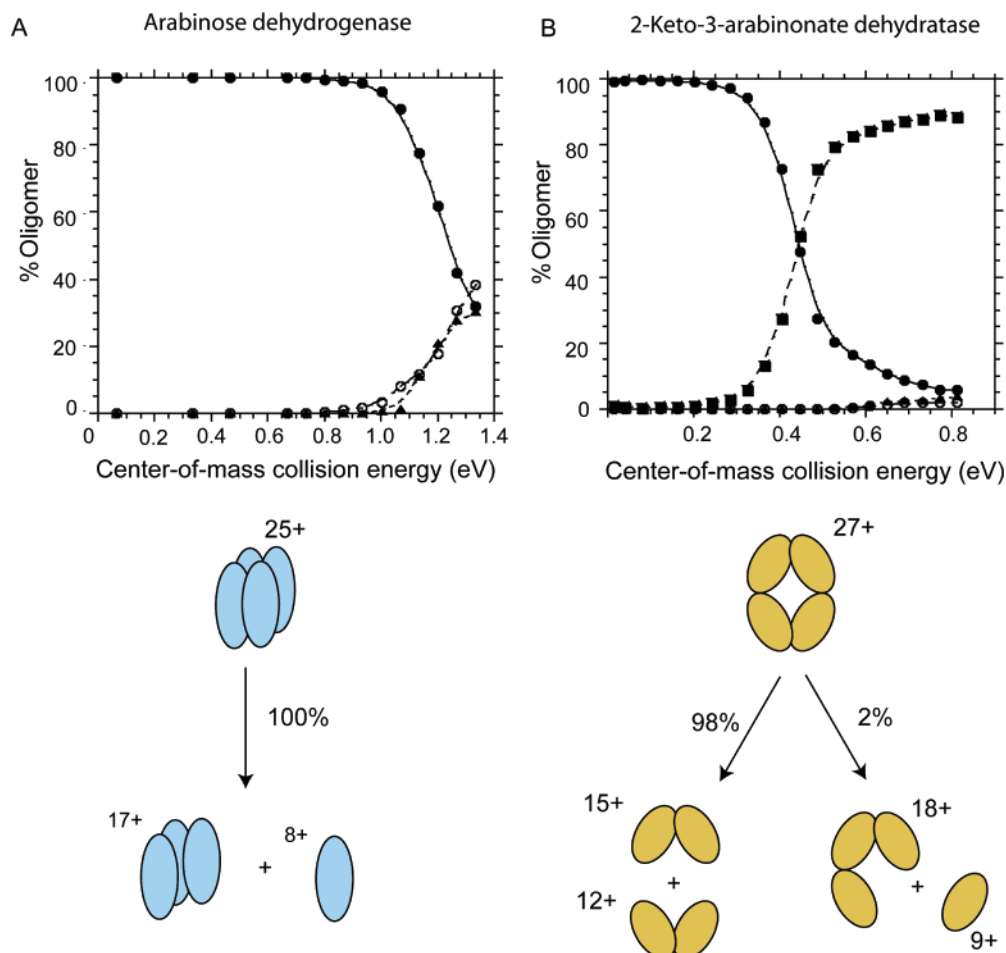


**Figure 7.** Breakdown graphs of arabinose dehydrogenase and 2-keto-3-deoxyarabinonate dehydratase tetramer ions. (A) Dissociation pattern of arabinose dehydrogenase and (B) dissociation pattern of 2-keto-3-deoxyarabinonate dehydratase. Tandem mass spectrometry was performed on the  $27^+$  and  $25^+$  ion of 2-keto-3-deoxyarabinonate dehydratase and arabinose dehydrogenase, respectively. Solid circles indicate tetramer, open circles indicate trimer, solid squares indicate dimer, and solid triangles indicate monomer. At the bottom, the dominant pathways observed in the gas-phase dissociation of these two protein tetramers are summarized.

information can be obtained from gas-phase dissociation experiments of protein complexes. The many studies on this topic suggest that gas-phase dissociation is a process that is not directly related to solution-phase structure. Still, it has been shown that gas-phase dissociation experiments may still reflect, to some extent, quaternary structure characteristics of biomolecules.<sup>12,29,34–42</sup> For instance, gas-phase dissociation experiments of GroEL

chaperones in complex with unfolded polypeptide substrate molecules only showed dissociation of GroEL subunits, whereas the substrate molecules had a lower molecular mass and were partly in the unfolded state.<sup>42</sup> These results are in line with observations that substrate molecules bind to GroEL in a solvent-protected cavity, thereby possibly also preventing the substrate from being eliminated in the gas-phase dissociation. Furthermore, it has been shown that the 11-membered ring topology of the tryptophan RNA binding protein could also be maintained within a mass spectrometer and that the binding of a tryptophan molecule enhanced the complex stability.<sup>43</sup> Moreover, for double-stranded DNA, it has been suggested that the Watson–Crick base-pairing is preserved in the gas phase, although the helical structure is essentially lost.<sup>41</sup> Blackbody infrared radiative dissociation experiments showed that complementary DNA duplexes have an increased gas-phase stability, as compared to noncomplementary duplexes, that loss of adenine occurred only for noncomplementary duplexes, and that a correlation exists between the activation energy for dissociation of the duplex and the dimerization enthalpy in solution.

- (34) Benesch, J. L. P.; Sobott, F.; Robinson, C. V. *Anal. Chem.* **2003**, *75*, 2208–2214.
- (35) Chen, Y. L.; Campbell, J. M.; Collings, B. A.; Konermann, L.; Douglas, D. J. *Rapid Commun. Mass Spectrom.* **1998**, *12*, 1003–1010.
- (36) Gross, D. S.; Zhao, Y. X.; Williams, E. R. *J. Am. Soc. Mass Spectrom.* **1997**, *8*, 519–524.
- (37) Hunter, C. L.; Mauk, A. G.; Douglas, D. J. *Biochemistry* **1997**, *36*, 1018–1025.
- (38) Loo, J. A.; He, J. X.; Cody, W. L. *J. Am. Chem. Soc.* **1998**, *120*, 4542–4543.
- (39) Rostom, A. A.; Fucini, P.; Benjamin, D. R.; Juenemann, R.; Nierhaus, K. H.; Hartl, F. U.; Dobson, C. M.; Robinson, C. V. *Proc. Natl. Acad. Sci. U.S.A.* **2000**, *97*, 5185–5190.
- (40) Schwartz, B. L.; Bruce, J. E.; Anderson, G. A.; Hofstadler, S. A.; Rockwood, A. L.; Smith, R. D.; Chilkoti, A.; Stayton, P. S. *J. Am. Soc. Mass Spectrom.* **1995**, *6*, 459–465.
- (41) Schnier, P. D.; Klassen, J. S.; Strittmatter, E. F.; Williams, E. R. *J. Am. Chem. Soc.* **1998**, *120*, 9605–9613.
- (42) van Duijn, E.; Simmons, D. A.; van den Heuvel, R. H.; Bakkes, P. J.; van Heerikhuizen, H.; Heeren, R. M.; Robinson, C. V.; van der Vies, S. M.; Heck, A. J. *J. Am. Chem. Soc.* **2006**, *128*, 4694–4702.

- (43) Ruotolo, B. T.; Giles, K.; Campuzano, I.; Sandercock, A. M.; Bateman, R. H.; Robinson, C. V. *Science* **2005**, *310*, 1658–1661.

When we compared the quaternary structures of arabinose dehydrogenase and 2-keto-3-deoxyarabinonate dehydratase, as measured by X-ray crystallography, we found the main differences in the number of subunits contacting the other subunit in the tetramer. Whereas each arabinose dehydrogenase subunit interacts with three subunits, each 2-keto-3-deoxyarabinonate dehydratase subunit interacts with only two subunits. The monomeric masses of the two proteins are very similar, and the two protein complexes obtain a very similar number of charges during the electrospray process (average number of charges are 25<sup>+</sup> and 27<sup>+</sup>, respectively). We speculate that there is a relationship between the different topologies of the two tetramers and their gas-phase dissociation behavior. Apparently, the donut-shaped structure of 2-keto-3-deoxyarabinonate dehydratase is relatively unstable in the gas phase and requires less energy to dissociate into two dimers than into an unfolded monomeric and a trimeric species.

## CONCLUSIONS

In this paper, we report on the low-cost modification and optimization of a first generation Q-TOF 1 whereby we enhance the instrument's capabilities to perform gas-phase dissociation experiments of macromolecular systems, such as large proteins and protein complexes. The modifications in the first hexapole ion guide, ion-selecting quadrupole, collision cell, and TOF analyzer yielded a tandem mass spectrometer that offers excellent possibilities to study protein stoichiometries and gas-phase stabilities of large macromolecular complexes (Figure 1). The combination of an increased pressure in the ionization chamber and the locally increased pressure in the first stage of the hexapole ion bridge allowed the efficient cooling of large protein ions. We demonstrated experimentally that the low-frequency quadrupole allows ion isolation of ions up to  $m/z$  12 800 (theoretically 30 000) and that the decreased repetition rate of the TOF analyzer allows analysis of ions up to  $m/z$  38 150 (theoretically  $m/z$  58 000). The

modifications can be applied on every Q-TOF instrument and extend the possibilities of the instrument for macromolecular mass spectrometry significantly. In our opinion, the modified Q-TOF 1 is of interest to everyone working in the field of macromolecular mass spectrometry and more generic structural biology. The obtained results of the different protein complexes indicate the potential and limitations of gas-phase dissociation experiments to probe complex topologies and quaternary structures. In particular, our data generated on 2-keto-3-deoxyarabinonate dehydratase presents a thus-far unprecedented new mechanism in the dissociation of protein oligomers in the gas phase and adds to the current debate about whether gas-phase structures of protein complexes resemble those present in solution. We realize that our study forms only a starting point to answer this question. Therefore, in future studies, it will be essential to systematically study the dissociation pathways of different protein oligomers to probe the general applicability of the presented technique to study topologies.

## ACKNOWLEDGMENT

This work was supported by The Netherlands Organization for Scientific Research (NWO) (VENI 700.54.402) to R.H.H.vdH and by the Foundation for Fundamental Research on Matter (FOM) (01FB12) to E. vD. We thank The Netherlands Proteomics Centre for financial support. Jan Commandeur (MSVision) is thanked for excellent technical assistance, and Dave Langridge (MS Horizons), for the GroEL simulations in the hexapole ion bridge. We thank Saskia van der Vies (Vrije Universiteit Amsterdam) for critical reading of the manuscript.

Received for review June 7, 2006. Accepted August 22, 2006.

AC061039A